Thermal Performance & Flow Characteristics of Staggered in Reversed Arc-Shaped Roughness of Artificial Roughened Solar Air Heater

Surjeet Singh Rajpoot[1], Manish Singh Bharti[2], S. K. Nagpure[3], Sandeep Kumar Shah[4], Ankesh Kumar Pataskar[5]

[1,2,4,5] Mechanical Engineering, Rabindranath Tagore University Bhopal, MP, India,464993
[3] Mechanical Engineering, Scope Global Skills University Bhopal, MP, India, 462047
surjeet1458@gmail.com

Abstract. This research investigates the flowing appearances in a solar air heater utilizing a gap reverse arc pattern integrated with staggered elements. The investigation was carried out with some roughness parameters and also arc inclination (α) of 600, 0.4 relative staggered rib pitch (p'/p), 1 the relative gaping width (g/e). The relative roughness height (e/D_h) was 0.0452 from a measurements. Reynolds numbers were varied systematically over a range 3000-15000 and relative roughness pitch, p/e, had taken through about 6-12. The test section was consisted of four plates which have reverse arc gap and staggered rib simulation on the surface. The hydrodynamic and thermal impact caused by this configuration was compared to plain ducts with staggered rib turbulators. The heat transfer and frictional performances were also improved markedly by the reverse gap arc arrangement with the counter flowed element arrays. Namely, the friction factor and Nusselt number were 3.89 and 2.19 times enhanced associate to plain duct. Comparative improvements were also witnessed in comparison to non-arc staggered configurations, thus attesting to the efficiency of reverse arc gap design, as it was capable of inducing turbulence and deflecting Thermoboundary layers for better thermal performance.

Keywords: Friction Factor, Nusselt Number, Reverse arc roughness, Staggered element, Thermal performance.

1. Introduction

The increasing demand on renewable energy, solar thermal systems have become increasingly popular for enabling less reliance on conventional fossil fuels of these, solar air heaters (SAHs) is widely used to heat spaces, dry crops, and industrial process preheating because of their simple design, low maintenance requirements and their environment-friendliness. However, a key drawback of traditional SAHs is their intrinsically low thermal performance, mainly attributed to the little diffusion of heat characteristics b/n the absorber surface and air flow, [1].

For promoting heat transfer in these SAHs, customizable HTS devices are probably required; an effective technique for this is enhancing the surface thermal concert of the absorber. These basics can generate wave, interrupt laminar sub layer and in-

R. Vasanth Kumar Mehta et al. (eds.), *Proceedings of the International Conference on Intelligent Systems for a Sustainable Future (ISSF 2026)*, Atlantis Highlights in Intelligent Systems 16,
https://doi.org/10.2991/978-94-6239-693-7_32

crease convective heat transfer coefficient. Examples of such roughness geometries are ribs, grooves and protrusions in different arrangements. Ribbed surfaces have received special attention in reducing heat transfer rates with increased friction drop; however, the drop due to ribs was so substantial that it suffered a lot in every sense. The significance of rib structure, alignment, and configuration on flow and temperature transferring behaviour has been studied in recent research. Staggered rib constructions optimize performance by improve net mixing and secondary flows.

Furthermore, innovative designs such as arc-shaped and gapped ribs have been introduced to further enhance turbulence while aiming to augment the steadiness between heat transfer augmentation and drop of pressure, [2].

The available reversal of arc shaped gap with staggered ribs researches in the open literature find new reversed arc-shaped gap is announced and an experiment research has been conducted to examine its impact on thermal hydraulic concert for a solar air heater duct. These designs are intended toward enhance turbulence intensity and more efficiently disturb thermal boundary layers compared to traditional rib configurations. To examine the performance, an experiment investigation was carried out of presented design configuration as affected by changes in Reynolds number and geometry. This continued to be compared in the case of the plain ducts and for conventional staggered ribbed surfaces to additional transitions in the friction factor with the Nusselt number. This study is very helpful in setting the design parameters of artificial roughness aimed at an efficient solar air heaters.

Despite of simply maximizing Nusselt number, recent research have focused on modifying rib geometry for improved thermo-hydraulic performance found that applying reverse NACA-profile ribs under turbulent flow parameters raised heat transfer[2, 3]. Researchers have demonstrated that while keeping minimal friction penalties, flexible circular ribs improve mixing intensity. More recent work [4] demonstrated that providing gaps to the transverse wire ribs significantly enhances thermo-hydraulic behavior. Reverse arc-shaped ribs with staggered arrangements, particularly in the Reynolds number that lies between 3000–15000, have not yet been extensively investigated. By experimentally evaluating the thermal and flow behaviors of staggered reverse arc-shaped roughness elements, the present study intends to close this gap.

2. Roughness Profile

The rib-roughness used in this work is staggered pin short-sided and is organized such that there are reversely arc shaped ribs. The objective of this novelty design are to improve the instability and increase heat transmission rates in the solar air heater duct. Various geometric parameters were investigated in the study to their influence on thermo hydraulic concert. The relative roughened pitch (p/e) was adjusted to be 6 - 12 and the pitch ratio (p'/p) representing the distance between staggered ribs to rib pitch, to be 0.4. The ratio of hydraulic diameter was kept constant ($e/D_h = 0.0452$). A

reversal arc angle (α) of 60° was applied for reversed arc ribs, to induce the return flow into a curved reverse flow path, leading to improvement in the fluid heating surface interaction. Furthermore, the g/e was kept at 1. All these parameters contribute to the particular structure of the roughness elements considered in this work and reported in Tab. 1.

3. Laboratory Performance

3.1 Representation Layout

The experimental setup aimed at evaluating rough absorber consisted of a rectangular channel fabricated from 25 mm thick plywood with complete length of 2350 mm and constant elevation (H) of 25 mm. The channel was divided into four main sections:

1. **Inlet section**: 800 mm in length with hydraulic diameter (Dh) of 17.33 mm
2. **Test section**: 1000 mm in length with Dh of 21.66 mm, housing the roughened absorber
3. **Outlet section**: 550 mm in length with Dh of 11.91 mm
4. **Transition/mixing section**: Fitted with internal baffles for uniform temperature distribution

The absorber in order for better thermal performance, the test portion's bottom surfaces was specifically roughened to various relative roughened pitch (p/e) values (6, 8, 10, and 12) and had a thickness of 1.2 mm. The investigational setup is illustrated in Fig. 1.

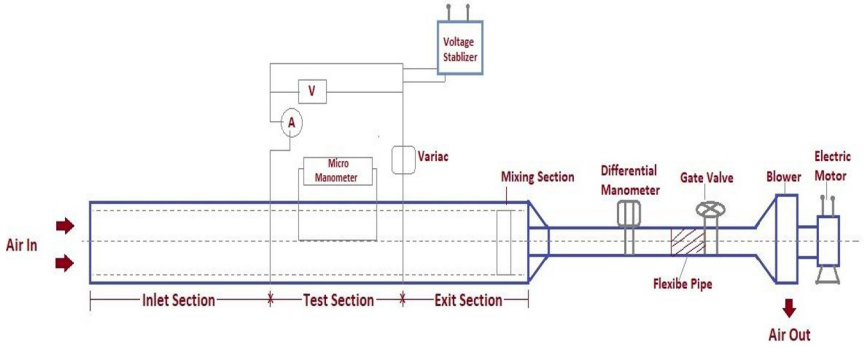

Fig.1 Representation diagram of set-up

3.2 Test Rig Configuration

The arrangement used for research of friction factor and heat transfer coefficient comprises an entrance and a duct, test then leaving segments, a blow feeder, a regulator tap, a calibrated orifice-meter, heating arrangement and temperature measuring device. The air passes in from surroundings over entering of the channel. The duct's opposite end is duct is coupled towards a blower over globular pipeline and conversion segment. A standardized orifice-meter are delivered on the channel in-

tended for capacity of airflow proportion. A U-tube vertical manometer taking water by way of mano-metric fluid usages toward degree the pressure drops transversely orifice-meter. To monitor the plate temperatures at different points, thermocouples with copper wires were utilized. The data from these thermocouples was recorded with a digital voltmeter. A Variac was used to deliver a heat flux ranging from 0 - 1000 W/m². Additionally, using a micro-manometer engaged towards assess pressure fall through the experiment segment.

3.3 Heating and Insulation

An electric heater using nichrome wire mounted on an asbestos sheet provided heat to the test section. The top of the heating unit was covered by glass wool insulation to reduction in heat loss. The entire assembly was thermally insulated using 50 mm thick Thermo-cool insulation. The GI duct section leading to the orifice was wrapped with standard rope insulation

3.4 Air Flow System

Air was drawn from the atmosphere by a fan. Mass flow rate was controlled manually using a shut-off valve. The outlet connected to an 80 mm diameter GI duct through a transition section. An orifice plate was used for flow measurement.

3.5 Measurement Instrumentation

Digital pressure gauge used to conclude airflow rate, digital micro-manometer noted pressure drop through the experiment section. Thermocouples monitored temperature distribution. Data acquisition system logged all temperature data. Thermocouple arrangements are one thermocouple near the entrance to measure inlet air temperature. Five thermocouples uniformly spaced across the duct area for outlet temperature. Fourteen thermocouples strategically placed along the absorber plate

3.6 Testing Procedure

All thermocouples were calibrated using a standard procedure with reference to a certified thermometer. Experiments were conducted at Reynolds numbers going starting 3,000 to 15,000. Data was recorded only under steady-state conditions, typically requiring 2 to 2.5 hours. Steady-state was defined as temperature at any monitored point remaining unchanged for five continuous minutes. The abilities of multiple roughness configurations was evaluated and compared with that of a smooth surface. For the investigation of the heat transfer growth and pressure reduction appearances for various surface roughed configurations, this comprehensive methodology assured accurate data acquiring.

3.7 Roughness Elements and Constraint Ranges

The configuration of artificial rib component, arranged on a distinct double arc in reverse, is shown in plot. It a 20 mm pitch (p) and an arc angle (α) 60^0. The profile of the roughed absorber plates is illustrated in Fig. '2'. Four different roughed plate were assembled then verified with varying gap (g), while maintaining a fixed roughened relative height (e/Dh). The parameter ranges are detailed in Tables 1. Additional patterns with dissimilar pitch values and arc angles were also evaluated.

Table-1 Range of constraints

Parameter	Range
Roughened Relative Pitch (p/e)	6 to12
Attack Angle (α)	60^0
Staggered relative rib pitch (p'/p)	0.4
Roughened relative height (e/Dh)	0.0452
Heat flux (I)	1000 W/m2K

4. Validation of experimental set-up

The standard empirical correlations for smooth plate behaviour formally incorporate them into section. For comparative analysis, thermal and frictional concert of rough absorber plate remained assessed against the corresponding values for a smooth plate using established empirical correlations.

The Nusselt number for a plain plate (Nu_s) was designed using the correlation, The calculation, $Nu = 0.023.Re^{0.8}.Pr^n$, is used to calculate Nusselt number for entirely established tempestuous stream in plain, globular pipes, where 'n' is 0.4 for warming and 0.3 for cooling.

$$Nu_s=0.023.(Re^{0.8}).\ (Pr^{0.4}) \quad (1)$$

The friction aspect for a smooth plate (f_s) was expected using the empirical relation:

$$f_s=0.085.(Re^{-0.025}) \quad (2)$$

5. Result & Discussion

5.1 Reduction and Investigation of Experimental Data

These baseline values (Eq. 1 and Eq. 2) were used to determine thermal-hydraulic enhancement down to surface roughness. The ratio of Nu/Nu_s and f/f_s provided insights into development in heat transfer comparative to increase in flow resistance.

Values of plate temp, in addition to air temp at the entering and passage, are restrained less than steady-state circumstances. Based on these temperatures and the pressure fall in the experiment section, the friction factor and Nusselt number is calculated through investigational statistics. Appropriate factors are derived by this analysis.

The heat gain by air is a crucial parameter, as it directly relates to the effectiveness of the system in transferring solar energy to air flow by duct. To calculate heat addition by air, you can use the following formula:

Heat Gain by Air

$Q_{air} = m \times c_p \times (T_{out} - T_{in})$ (3)

Reynolds Number, Re

$Re = \frac{VDh}{v}$ (4)

Established on investigational statistics, calculate Nu using

$Nu = \frac{h \, X \, Dh}{k}$ (5)

Heat transfer constant, h could be find out using:

$h = \frac{Qair}{As \, .(tp - tf)}$ (6)

Calculate friction factor using measured pressure dropping

$f = \frac{\triangle P. \; Dh}{2. \; L \, .\rho}$ (7)

5.2 Thermal-Hydraulic Concert (η):

The thermo–hydraulic effect factor (η) of the roughened absorber surface remained calculated to measure how much the heat transfer improved associated to rise in frictional resistance. This measure, known as the Effect Valuation Criterion (EVC), is stated as:

$\eta = [(Nu/Nu_s)/(f/f_s)^{1/3}]$ (8)

This ratio compares the enhanced heat transfer to the increased flow resistance and thus becomes fairly universal measure of overall performance. A value of η>1 means a net gain in thermal-hydraulic concert down to roughness elements at the topo the absorber.

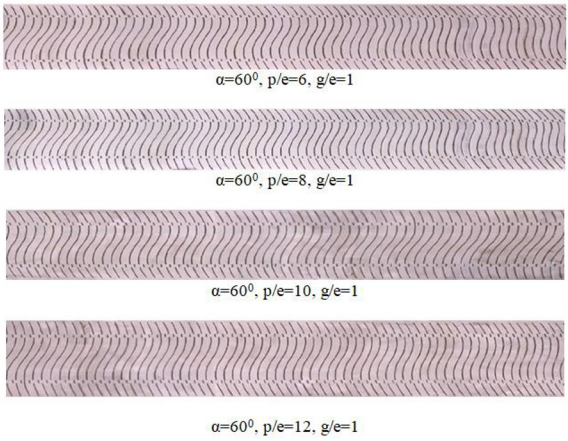

Fig.2 Roughed plates reversed arc shape

This chart relates Reynolds Number to Nusselt Number for several types of surface including; crossed ribs where the value of p/e is altered, and a smooth plate. For all cases with Re > 1 Nu grows like would expect, louder turbulence usually means more convective heat transfer.

Better heat transfer is shown by ribbed surfaces (with variable p/e values) have a significantly greater Nu than a smooth plate. The Nu of p/e = 10 is constantly the highest across ribbed surfaces, showing that it has the highest heat transfer capability. The heat transmission effectiveness slightly affects as p/e fluctuates from 10 (p/e = 6 to 12), illustrating that there is an optimal rib spacing. Heat transfer gets enhanced by ribbed surfaces comparing to a plain plate. For comparable conditions of flow, a p/e ratio of 10 provides a significant heat transfer (highest Nu) among the examined set-ups. This suggests that the heat transfer effectiveness during a turbulent flow in Figure 2 is substantially affected by the surface roughness characteristic (rib spacing). The Nusselt Number values fluctuate between around 20 to 160, where as the relative roughened pitch (p/e) ranges from around 6 to 12. The data basically indicates that optimized heat transport is measured by higher Nusselt numbers, which are associated with higher Reynolds numbers. There appeared to be a correlation involving the Nusselt number and relative pitch roughness with each Reynolds number. There may be a desirable roughness pitch for heat transfer efficiency, whereas the highest Nusselt numbers seem to be found at a middle p/e ratios (around 6–12). This graphic most likely originated from a study on heat transmission in pipes or channels with artificial roughness elements. This research examines how heat transfer performance fluctuates by the distance between roughness elements (in relation to their height) at different flow rates.

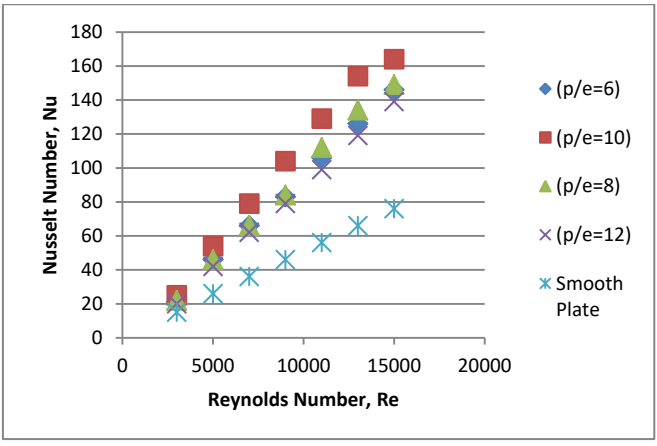

Fig.3 Deviations of Nu with Re of relative roughness pitch

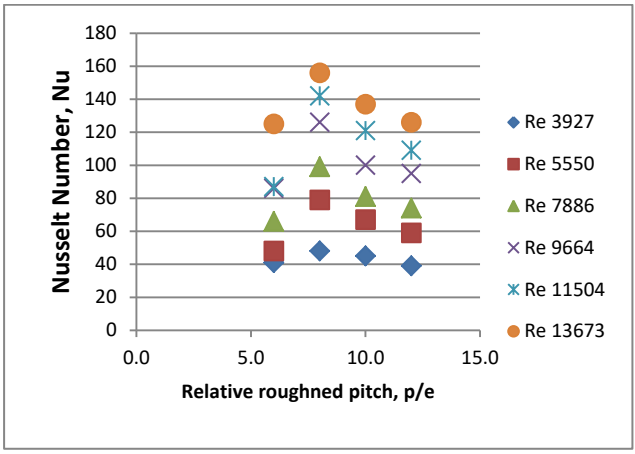

Fig.4 Deviations of Nu with relative gap width at few Reynolds number

Whereas the Nusselt Number Ratio varied between around 0 to 3.0, the Reynolds Number values fluctuated from around 3,000 to 15,000, respectively. The significant results from the graph illustrate that, with respect to the plain surface, all purposely roughened surfaces show greater heat transmission. A significant heat transfer enhance occurs in the p/e = 10.0 configuration. For every arrangement, the Nusselt Number Ratio appear to increase minimally on Reynolds Number. The Nusselt Number Ratio is lower on smooth surfaces, with values usually approximately 1.0 and 1.5. This graphic certainly illustrates the efficiency of heat transfer with varying surface roughness configurations as compared to a standard with a smooth surface. While compared to a reference circumstance shown in fig.4, the ratio Nu/Nus reflects the amount of better (or low) heat transmission.

The friction factor varies from from 0.000 to 0.030, whereas the Reynolds Number values vary from from 3,000 to 15,000 in addition. In accordance to the graph's observations, the plain plate has smaller friction factors with all roughed surfaces (all p/e values). The highest friction aspects values can be seen in the p/e = 10.0 configuration.

For every configuration, the friction factor tends to decline as the Reynolds Number increases. With consistent friction factor values of 0.010 or lower, this smooth plate achieves the lowest values. This graph certainly indicates that surface roughness effects flowing resistance in a fluid mechanics or heat transfer analysis. Higher values in fig.5 signify greater flow resistance. The friction characteristic is a dimensionless indication of the obstacle that fluid establishing across these surfaces faces.

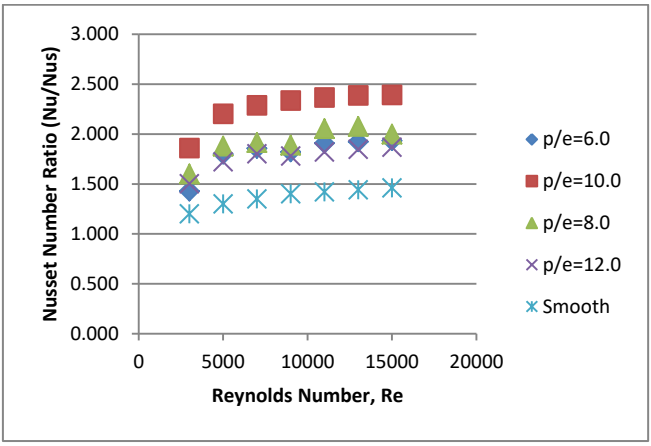

Fig.5 Deviations of Nu ratio with Re for different relative rib roughness pitch

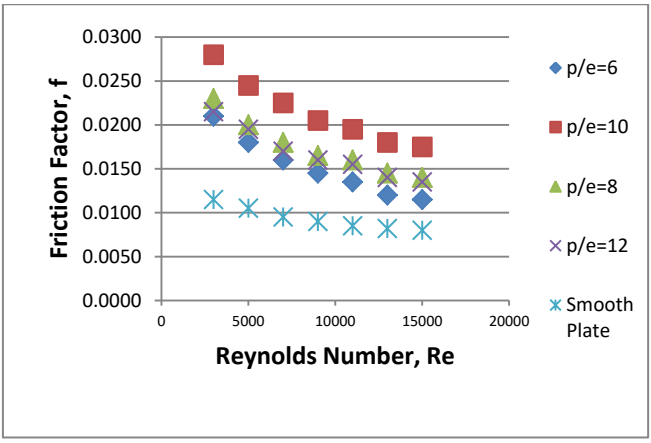

Fig.6 Graph of friction factor vs Renolds number

5.3 Comparative Discussion with Existing Literature

The analysis's highest Nusselt number augmentation (Nu/Nus = 2.19) is in agreement with outcomes for arc-shaped roughness geometries which have been reported previously.

In particular, concluded that symmetrical gap arc ribs produced a Nu enhance of around 2.1. In the same direction [5], the broken arc ribs improved thermal transfer by 1.8 to 2.3[6]. Comparing to transverse rib concepts described in, where friction enhancement was about 2.5–3.0, this particular reversed arc staggered structure generated a larger friction factor raise (≈3.89). Higher secondary vortices, attachment of separated flow, and improved disruptions of the thermal boundary layer being the reasons for this rise [7]. The research's optimum relative roughness pitch (p/e = 10) is in alignment with research, which indicated that peak thermo-hydraulic performance occurred with p/e values between 8 and 12. In comparison with normal transverse or

broken arc ribs, the reverse arc staggered configuration provides improved turbulence the growth overall, which results in higher thermal performance factor rates ($\eta > 1.5$) [8]. Significant secondary vortices and flow separation allowed the reversed arc staggered configuration to provide an increased friction factor, which is verified by comparable measurements in [9]. A Nusselt number increase of roughly 2.1 was observed in symmetrical gap arc ribs [10]. According to [11], the ideal roughness pitch ($p/e = 10$) indicates highest thermo-hydraulic performance within the range of 8–12.

6. Conclusion

Established on the exploration of experimental data presented in the plots:
1. As compared to a smooth duct, such staggered reverse arc-shaped roughness significantly improves heat transport, having a maximum Nusselt number augmentation of 2.19 times.
2. Enhanced turbulence the growth and separation of fluids were detected by the 3.89-fold raise in the friction factor.
3. The optimum thermo-hydraulic performance was found at $p/e = 10$, which also represents the optimum relative roughness pitch.
4. Within the investigated Reynolds number interval (3000–15000), the thermo-hydraulic performance coefficient (η) maintained over unity, indicating net performance growth.
5. The reversed arc staggered configuration results in enhanced boundary layer disruptions and stronger secondary flow formations when compared to previously circulated arc with broken rib configurations.
6. In solar air heaters, the roughness concept works well for applications that need enhanced thermal performance along with a sustainable pressure drop.

Acknowledgments. This study was supported by Rabindranath Tagore University, Bhopal. The authors gratefully acknowledge the support provided by the Department of Mechanical Engineering for facilitating the experimental setup and laboratory resources required for this research.

Disclosure of Interests. The authors declare that they have no competing interests to disclose that are relevant to the content of this article.

References

1. R. Singh and R. Narayanan, “Comprehensive review of thermal and thermohydraulic performance in solar air heaters with advanced artificial roughness geometries,” Energies, vol. 18, no. 23, Art. no. 6157, 2025.
2. S. Kumar and R. K. Das, “Comparative study of NACA 0020 profile ribs in forward and reverse flow solar air heater,” Case Studies in Thermal Engineering, vol. 34, 2022, Art. no. 102015.
3. G. K. Chhaparwal, R. Goyal, A. Srivastava, A. Goyal, A. D. Oza, M. I. H. Siddiqui, L. Natrayan, L. Kumar, and S. Chandrakant, “Numerical and experimental investigation of

a solar air heater duct with circular detached ribs to improve its efficiency," Case Stud. Therm. Eng., vol. 60, p. 104780, 2024.
4. D. S. Mondal et al., "Thermo-hydraulic enhancement of solar air heater using modified transverse rib with gap," Solar Energy, vol. 258, pp. 113856, 2025.
5. J. Ambade and A. Lanewar, "Experimental investigation of solar air heater with modified arc rib roughness," International Journal of Thermal Sciences, vol. 164, 2021, Art. no. 106892.
6. S. Singh and R. S. Gill, "Heat transfer and friction characteristics of staggered rib roughened solar air heater duct," Solar Energy, vol. 221, pp. 412–425, 2021.
7. J. L. Bhagoria, , J.S. Saini, and S.C. Solanki, heat transfer coefficient and friction factor relations for a rectangular solar air heater duct with transverse wedge-shaped rib roughness on the absorber plate, Journal of Renewable Energy, Vol. 25, pp. 341-369, 2002.
8. V.S. Hans, R.S. Gill, Sukhmeet Singh, Heat transfer and friction factor correlations for a solar air heater duct roughened artificially with broken arc ribs, 14(8), (2017) 77-89.
9. Y. Agrawal, V. S. Pagey, and J. L. Bhagoria, "Thermo-hydraulic performance analysis of reverse arc ribs in a solar air heater," Materials Today: Proceedings, vol. 62, pp. 5120–5126, 2022.
10. A. Verma and D. S. Thakur, "Performance evaluation of gapped arc rib roughness under turbulent flow," Thermal Science and Engineering Progress, vol. 45, 2024, Art. no. 101945.
11. Rajpoot SS, Koli DK. CFD analysis of solar air heater duct with rectangular rib surface. Int. J. Eng. Trends Tech. 2013; 4: 3006-3011.